Hindawi
Wireless Communications and Mobile Computing
Volume 2022, Article ID 8206660, 13 pages
https://doi.org/10.1155/2022/8206660

Research Article

User Capacity Analysis of Space-Based Internet of Things with Multibeam Techniques

Zhenhua Zhang,[1,2] Siyue Sun,[1,2] Huiling Hou,[1] Lulu Zhao,[1] Guang Liang,[1,2] and Jinpei Yu[1,2]

[1]*Innovation Academy for Microsatellites of CAS, Chinese Academy of Sciences, Shanghai 200120, China*
[2]*University of Chinese Academy of Sciences, Beijing 100000, China*

Correspondence should be addressed to Siyue Sun; sunmissmoon@163.com

Received 27 May 2021; Accepted 16 September 2021; Published 29 April 2022

Academic Editor: Xin Liu

Space-based Internet of Things (S-IoT) utilizes the characteristics of satellite network coverage, strong antidestructiveness, and full-time work to realize large-scale sensing and interconnection of everything in the sky, land, sea, and air. The user capacity of S-IoT satellites is mainly determined by beam design, communication schemes, satellite-to-earth links, and communication protocols, which directly affect the system capacity and operational capabilities of S-IoT. This paper proposes an S-IoT satellite user capacity analysis model with multibeam and spread spectrum technology. Taking into account the randomness of user distribution, the difference in transmit power, and different spreading sequences, the user capacity of S-IoT satellites was simulated and compared in different scenarios. Based on these results, this article analyzes the key factors affecting user capacity, which will provide a valuable reference for S-IoT design, link optimization, and power selection.

1. Introduction

With the increase in demand for Internet of Things applications worldwide and the expansion of the scale of the industry, the service capabilities of the Internet of Things are limited by the small coverage, poor adaptability, and fragility of terrestrial communication networks. As a result, the problem of the mismatch between the service capabilities of the terrestrial Internet of Things and the demand has become increasingly prominent. Compared with terrestrial communication networks, satellite communication networks have the advantages of wide coverage, strong antidestructiveness, and full-time work, which can realize large-scale perception and interconnection of all things in the sky, air, sea, and earth [1].

Attracted by the huge market for the Internet of Things, there is a global trend to develop satellite communication networks, making space-based Internet of Things (S-IoT) services possible to bridge the gap between the above capabilities and needs, such as Iridium and Globalstar. In addition, dedicated S-IoT solutions such as Orbcomm, ARGOS, and Tianqi systems have also been released one after another [2–5].

S-IoT user access to the wireless network is a typical multiuser communication system, which mainly realizes data collection, monitoring, and control of sensors and other equipment deployed in space, air, ground, and sea. Due to the characteristics of the Internet of Things business, the wireless access network pays more attention to user capacity rather than data rate. Moreover, considering the wide-area coverage characteristics of space-based systems, the coverage of an S-IoT node is more than a dozen terrestrial nodes. On the other hand, frequency resources have become one of the main constraints restricting the construction and deployment of satellite communication systems, and the limited spectrum resources have been continuously occupied with the continuous growth of satellite communication system planning. Therefore, achieving user capacity under limited bandwidth and power constraints is one of the key factors for S-IoT to ensure service capabilities and market share [6–8].

This paper proposes an S-IoT communication system model with space division multiplexing (SDM), frequency division multiplexing (FDM), and code division multiple access (CDMA). Based on this model, the multiple access scheme and communication protocol corresponding to the S-IoT uplink user link communication system are analyzed. Taking into account the randomness of user distribution, the difference in transmit power, and different spreading sequences, the user capacity of S-IoT satellites was simulated and compared in different scenarios. Based on these results, this article analyzes the key factors affecting user capacity and provides valuable references for the design and optimization of S-IoT systems.

2. Multi-beam Multi-user S-IoT System Model

S-IoT is a comprehensive information system that is based on the space-based information network and provides interactions between things and things, people and things, and people and people. It mainly provides data transmission services for nodes in areas that are difficult to cover by terrestrial networks, such as forests, oceans, and deserts, as well as nodes in special areas, such as disaster areas and battlefields [9].

As shown in Figure 1, S-IoT consists of two parts: a space segment and a ground segment. The space segment is composed of low earth orbit satellites (LEO)/geostationary orbit satellites (GEO), which provide services for the ground segment through various link transmissions. The ground segment is composed of various IoT terminals, through which sensors are used for information interaction [10, 11]. Taking into account the limited spectrum resources, changing communication conditions, and higher user capacity requirements, the satellite multibeam uplink communication system considered in this article uses CDMA. Users access the same satellite with the same spreading sequence while they are multiple accessed by different phases of the spreading sequence resulting from random transmitting time and different transmitting delay in the space-based receiver. Therefore, the relative characteristics of the spread spectrum sequence used will affect the performance of the S-IoT communication system. On the other hand, in view of the wide coverage of S-IoT satellites, the high gain of the receiving antenna, and the increase of user capacity, fixed multibeam antenna technology is adopted. In order to reduce interference and increase user capacity, adjacent beams can use different carrier frequencies.

In this paper, the signal to interference plus noise ratio (SINR) of the received signal at the receiver of the satellite is analyzed to evaluate the user capacity of the S-IoT system in different communication scenarios. The SINR of user k can be calculated as follows:

$$\mathrm{SINR}^{(k)} = \frac{E_b}{I_0 + N_0} = \frac{\mathrm{EIRP}^{(k)} - L_f^{(k)} - L_0^{(k)} + G(\theta_k, \varphi_k) - L_m}{(I_0 + N_0)R_b}, \tag{1}$$

where $\mathrm{EIRP}^{(k)}$ is the equivalent isotropically radiated power which is determined by the transmission power, the antenna transmission gain, and the terminal transmission loss of user k. $L_f^{(k)}$ is the free space transmission loss which is determined by the frequency of carrier and the distance between the user terminal and the satellite. $L_0^{(k)}$ is the other loss including polarization loss and rain attenuation. $G(\theta_k, \varphi_k)$ is the receiving antenna gain which is determined by the azimuth and pitch angles between the user terminal and the satellite. L_m is the demodulation loss of the receiver. I_0 is the power spectral density of noise, and R_b is the bit rate. I_0 is the power spectral density of interference which is mainly affected by the multiuser interference (MUI) resulted from poor correlation property of the spreading code employed by the S-IoT.

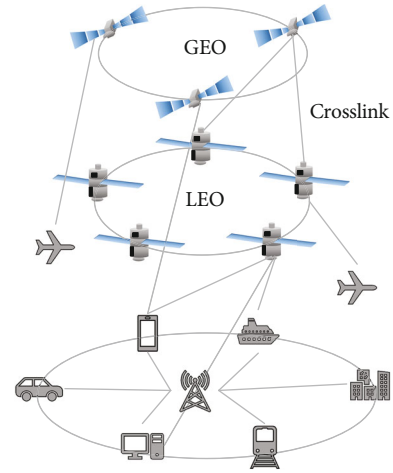

Figure 1: System model of S-IoT.

The following article will analyze the user capacity of the above system under different communication scenarios through theoretical derivation and simulation. In the multibeam satellite communication system, all terminal devices in the multibeam area use the reverse link to transmit the requested data to the multibeam satellite through the transmitting antenna. The multibeam satellite receives and amplifies the signal, forwards it to the gateway through the reverse link, and transmits it to the ground network for processing. After the processing is completed, the reply data is transmitted to the gateway station, and the reply data is sent to the multibeam satellite using the forward link, and it is also amplified and transferred to the multibeam area, thus completing the data request and receiving process [12, 13].

3. User Capacity Analysis

3.1. The Spreading Sequences. In a S-IoT based on the spectrum spreading technique, the chip rate is generally constant since the authorized bandwidth is limited and fixed. Therefore, different data rates will result in those different lengths of the spreading sequences should be employed, which will bring different effects on user capacity [14–17].

In classical spread spectrum systems, two kinds of spreading schemes can be employed: scheme 1—short spreading sequence scheme—and scheme 2—long spreading

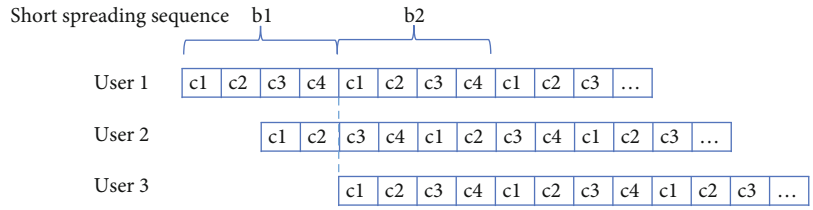

Figure 2: Scheme 1—short spreading sequence, taking spreading gain = 4 as an example.

sequence scheme. As shown in Figure 2, each bit of data of each user uses the same spreading code in scheme 1. Therefore, MUI is determined by different phases of the spreading sequence caused by random transmitting time and different transmitting delay in the space-based receiver. Due to the limited length of the spreading sequence, the probability of collision (data arrived at the same chip phase) is very high which becomes the main factor affecting the user capacity. In order to reduce the collision probability, the long spreading sequence scheme can be employed, as shown in Figure 3, where different bits of each user are successively spread by a long spreading sequence. In this situation, the correlation properties of the chips within different bits will be various, since only a short part of the spreading sequence is used to realize code division multiple access. The MUI of scheme 2 will be more random and difficult to quantify. According to the above analysis, the following article will focus on analyzing the collision probability of the system with short spreading sequence and on analyzing the MUI of the system with long spreading sequence.

3.2. Collision Probability of the System with Short Spreading Sequence. In a CDMA system using short spreading sequence communication, if multiple users are located at similar address codes, interference between multiple users can not be avoided, which will affect the quality of information transmission of the entire system [18, 20].

Suppose the number of users is k, and the users interact with each other in the multibeam satellite communication system. Random transmitting time and different transmitting delay will result in different arrived chip delay of each user $\tau \in \{1, 2, \cdots, \mathrm{N}\}$, where N is the length of the spreading code. The definition of collision is as follows: if the chip delay between 2 or more users is less than 4, it will be counted as a collision. In addition, since there is cyclicality in the definition, when $\tau_1 = 1$ and $\tau_2 = N$, it is also counted as collisions.

According to the principle of probability statistics, the collision probability P can be obtained.

$$P = 1 - \frac{(N - 3k - 1)!}{N^{k-1}(N - 4k)!}. \tag{2}$$

The access probability in the case of collision is defined as the ratio of the number of users which can communicate to the total user number. This paper uses the Monte Carlo random method to simulate the collision access probability.

First, a $k * 1$ matrix is randomly generated, and the elements in the matrix are randomly selected from 1 to N, and then, the average collision access probability of the user is calculated in ten thousand times random experiments. The angle mark is the corresponding spreading gain. The results are as follows, where spreading gain is assumed to be 512, 256, 128, and 64, respectively.

As is shown in Figure 4, the collision access probability decreases with the increase of the number of users with the same spreading gain, and it decreases with the increase of spreading gain with the same number of users.

3.3. MUI of the System with Long Spreading Sequence. Different from the scenario with short spreading sequence where the user capacity is mainly determined by the probability of collision, MUI becomes the main factor affecting the user capacity in the scenario with long spreading sequence [21, 22]. In such scene, the access probability refers to the probability that the user's SINR is greater than the threshold under the statistics of users at different information rates and different terminal powers [23, 24].

The calculation method of SINR is as follows:

(1) Calculate the entrance level P_r of each user according to the transmit power, position, and beam gain of each terminal (beam gain is imported from simulation results of antenna gain pattern, and the terminal position is random)

(2) Calculate N_0 based on receiver thermal noise shown as

$$N_0 = -228.6 + 10 \log \{10[1000(T_{\mathrm{a}} + T_{\mathrm{r}})]\}, \tag{3}$$

where T_{a} is the antenna noise temperature and T_{r} is the receiver equivalent noise temperature

(3) Calculate the SINR of each user, and the MUI power density I_0 is

$$I_0 = \sum_{k=1, k \neq g}^{K} P_r * \frac{I}{R_b} \tag{4}$$

P_r is the transmit power, I is the correlation value, and R_b is the bandwidth before spreading. As mentioned above, the correlation properties of different bits are various since only a short different part of the spreading sequence is used to realize code division multiple access. We calculate correlation values in all possible chip delays of the employed

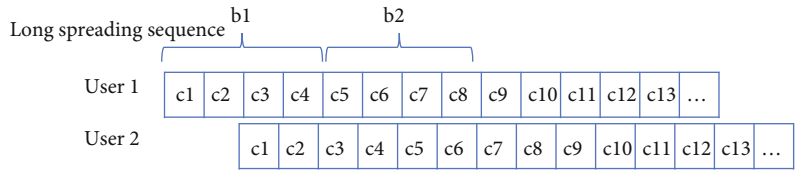

Figure 3: Scheme 2—long spreading sequence, taking spreading gain = 4 as an example.

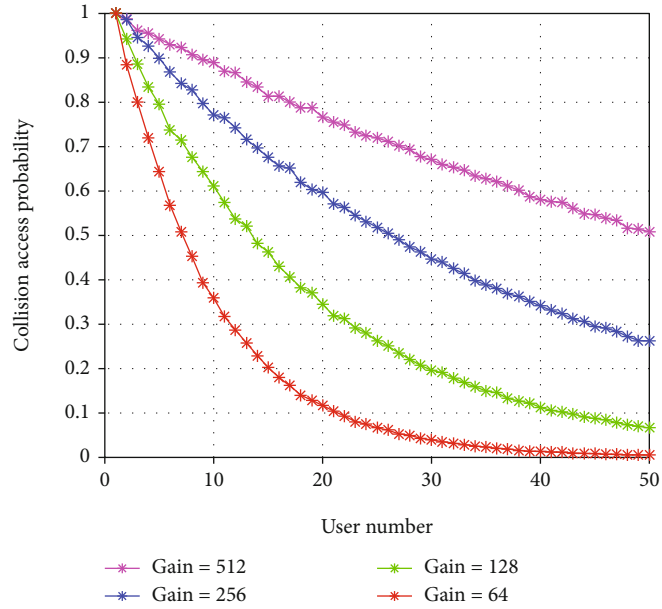

Figure 4: Collision access probability result graph.

Table 1: Long spreading sequence access probability in the average scene (SINR > threshold).

Power	512	256	128	64
P_0	0.8288	0.8288	$8.0000e-05$	0
$2 * P_0$	0.8473	0.8473	$1.6000e-04$	0
$6 * P_0$	0.8643	0.8643	$2.8000e-04$	0

Table 2: Short spreading sequence access probability in the average scene (SINR > threshold).

Power	512	256	128	64
P_0	1	1	1	0.9738
$2 * P_0$	1	1	1	0.9996
$6 * P_0$	1	1	1	1

sequence and take the average correlation value as I in equation (4) to simplify the evaluation [25].

4. User Capacity Simulation Results and Analysis

In this paper, the user capacity of a S-IoT satellite is evaluated under the assumption: (1) the satellite is equipped with 7 fixed receiving beams—one central beam evenly around with 6 edge beams; (2) the adjacent beams are assigned different carrier frequency to reduce interference; (3) the satellite is equipped with 50 receiving channels due to its limited bearing capacity.

In the simulation, the user position is randomly obtained according to the beam allocation, the spreading gain is assumed to be 64, 128, 256, and 512, respectively, and the transmit power of the user terminal have three levels: P_0, $2 * P_0$, and $6 * P_0$.

4.1. Capacity Analysis in the Average Scene. The average scene refers to an ideal average scene where the central beam is connected to 8 users and each edge beam is connected to 7 users. Finally, statistics are made on the probability that the user's SINR is greater than the threshold for 50 users at different rates and different terminal powers.

Tables 1 and 2 show the access probability in an average scene of 50 users when power control is not added.

From the comparison of Tables 1 and 2, it can be seen that the access probability of the short spreading sequence is higher than that of the long spreading sequence. Although short spreading sequences need to consider the impact of collisions on user capacity, the autocorrelation characteristics of short spreading sequences are better than long spreading sequences. Therefore, under the condition of higher spreading gain, the access probability of short spreading sequences is higher.

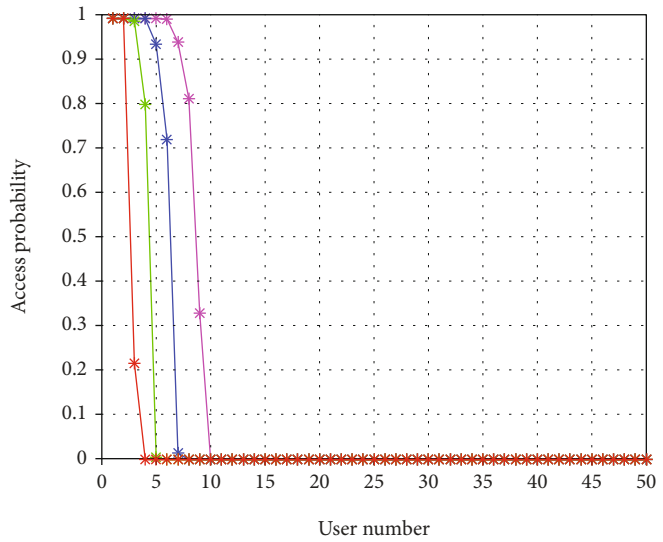

(a) Main beam

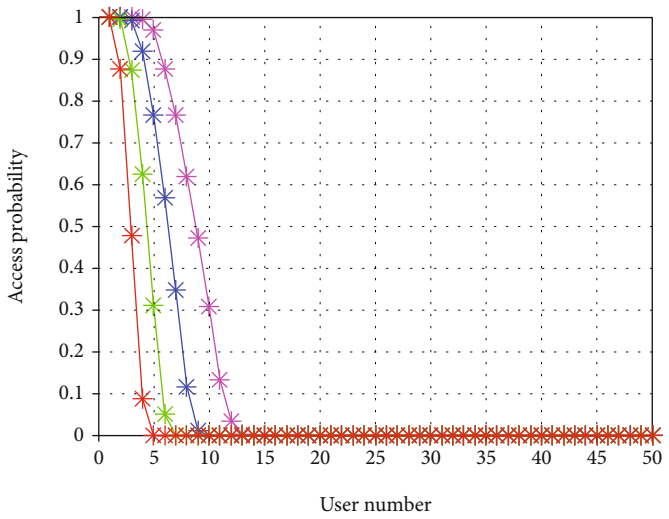

(b) Edge beam [50 : 0]

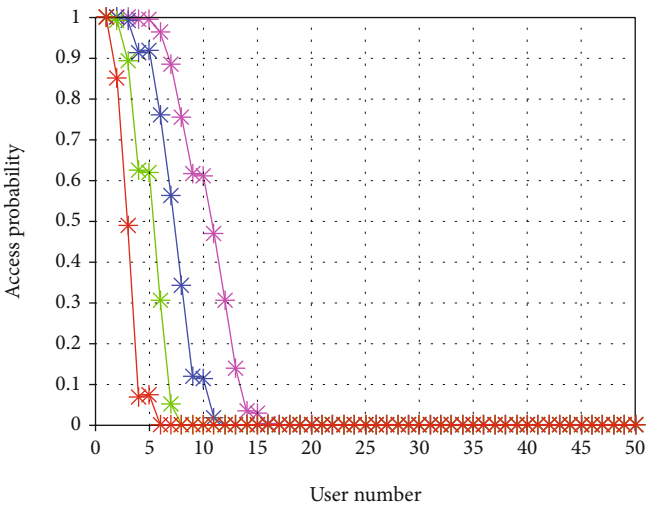

(c) Edge beam [40 : 10]

Figure 5: Continued.

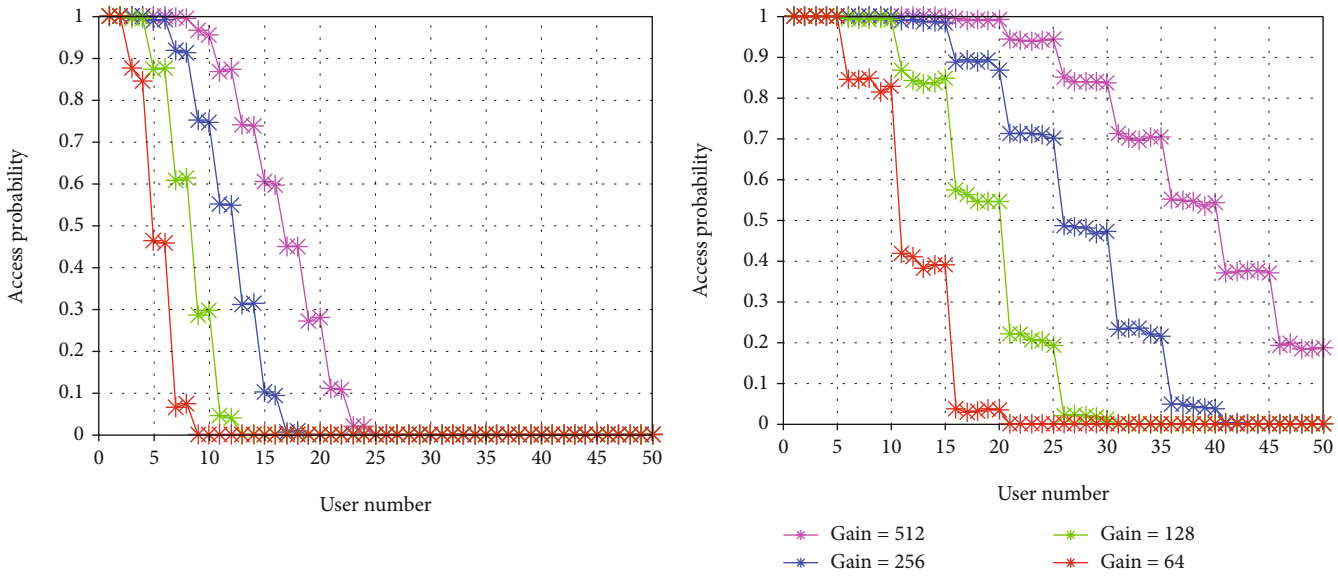

(d) Edge beam [25 : 25]

(e) Edge beam [10 : 40]

Figure 5: Terminal transmit power is P_0.

4.2. Single Beam Capacity Analysis

4.2.1. Beam Distribution. This section examines the capacity of a single beam. According to the beam and frequency allocation methods, if the impact of subchannel overlap is not considered, only interference exists between users of the same frequency channel. In the system design, the beam design will be completed based on the principle of equal flux coverage to ensure the beam gain within the satellite coverage. The simulation scenes in this section are divided into two types:

(1) Multiusers are accessed by the central main beam, and the user position is random

(2) Multiusers are accessed by edge beams with the same frequency. In the simulation, 50 users set different allocation ratios in the two selected edge beams, which are beam A and beam B. When the users are distributed in two beams, only the SINR of users in beam 1 are examined ([40 : 10] means that users 1, 2, 3, and 4 are distributed in beam A, user 5 is distributed in beam B, and so on)

4.2.2. Access Probability of Long Spreading Sequence. Since the frequency points of the main beam and the edge beam are different, the 6 edge beams are symmetrically equivalent and the same. Therefore, the capacity of the system under different user beam allocations can be obtained through the following single-beam capacity simulation results which are shown in Figure 5: terminal transmit power is P_0, Figure 6: terminal transmit power is $2 * P_0$, and Figure 7: terminal transmit power is $6 * P0$ (The angle mark is the corresponding spreading gain).

According to the simulation results, in the case of the same terminal transmitting power and in the same beam, user capacity increases as the spreading gain decreases. Only when 6 users access with a gain of 512 can the access probability of 90% be guaranteed. With a low gain of 64, only two users can be accessed while guaranteeing a 90% access probability. This is due to stronger multiple access interference in high-rate scenarios.

In the case of different terminal transmitting power when the gain is the same, user capacity increases with the increase of terminal transmission power. According to formula (2), the greater the terminal transmit power, the greater the interference power density, therefore, the greater the probability that the user is above the threshold. Increasing the power from P_0 to $6 * P_0$ ensures high access probability and can provide the capacity of 1 user (in the same beam).

4.2.3. Access Probability of Short Spreading Sequence. The simulation conditions in this chapter are consistent with the long spreading sequence.

According to the simulation results which are shown in Figure 8: terminal transmit power is P_0, Figure 9: terminal transmit power is $2 * P_0$, and Figure 10: terminal transmit power is $6 * P_0$, under the same power condition, the access probability of the main beam and the subbeam has different changing rates. It can be seen from Figure 8 that the coverage shape of the beam and the distance of the subsatellite point are different. Due to the near-far effect, the access probability of the word beams with the same shape and the same distance between the subsatellite points decreases slowly, while the main beam decreases at a faster rate. But while maintaining a high access probability (greater than 80%), the user capacity of the main beam is larger.

Consistent with the long spreading sequence, under the condition of the same beam and the same spreading gain, the user capacity increases with the increase of power. When the power is from P_0 to $6 * P_0$, 5 more users can be accessed when the access probability is above 90%. And in the same

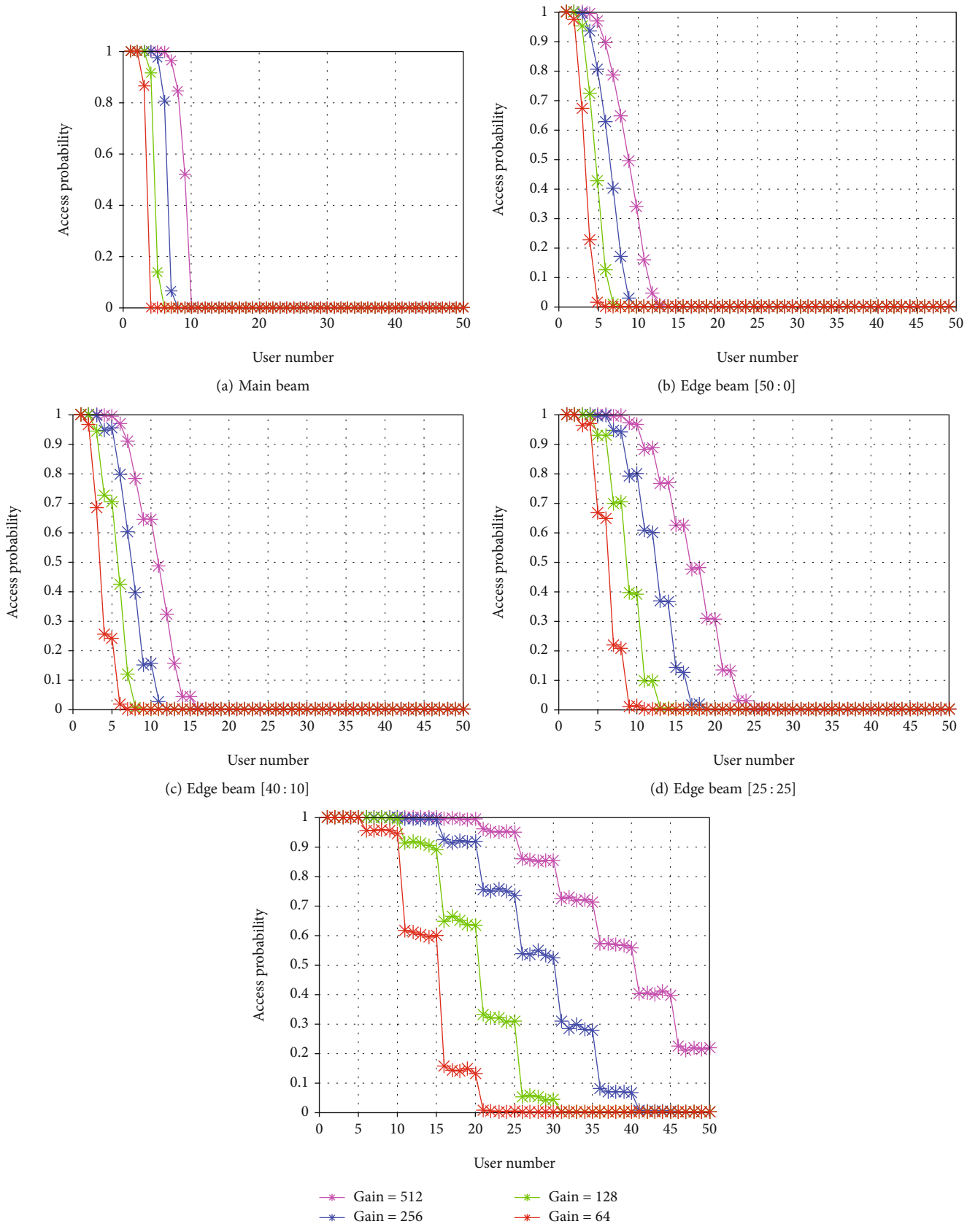

Figure 6: Terminal transmit power is $2 * P_0$.

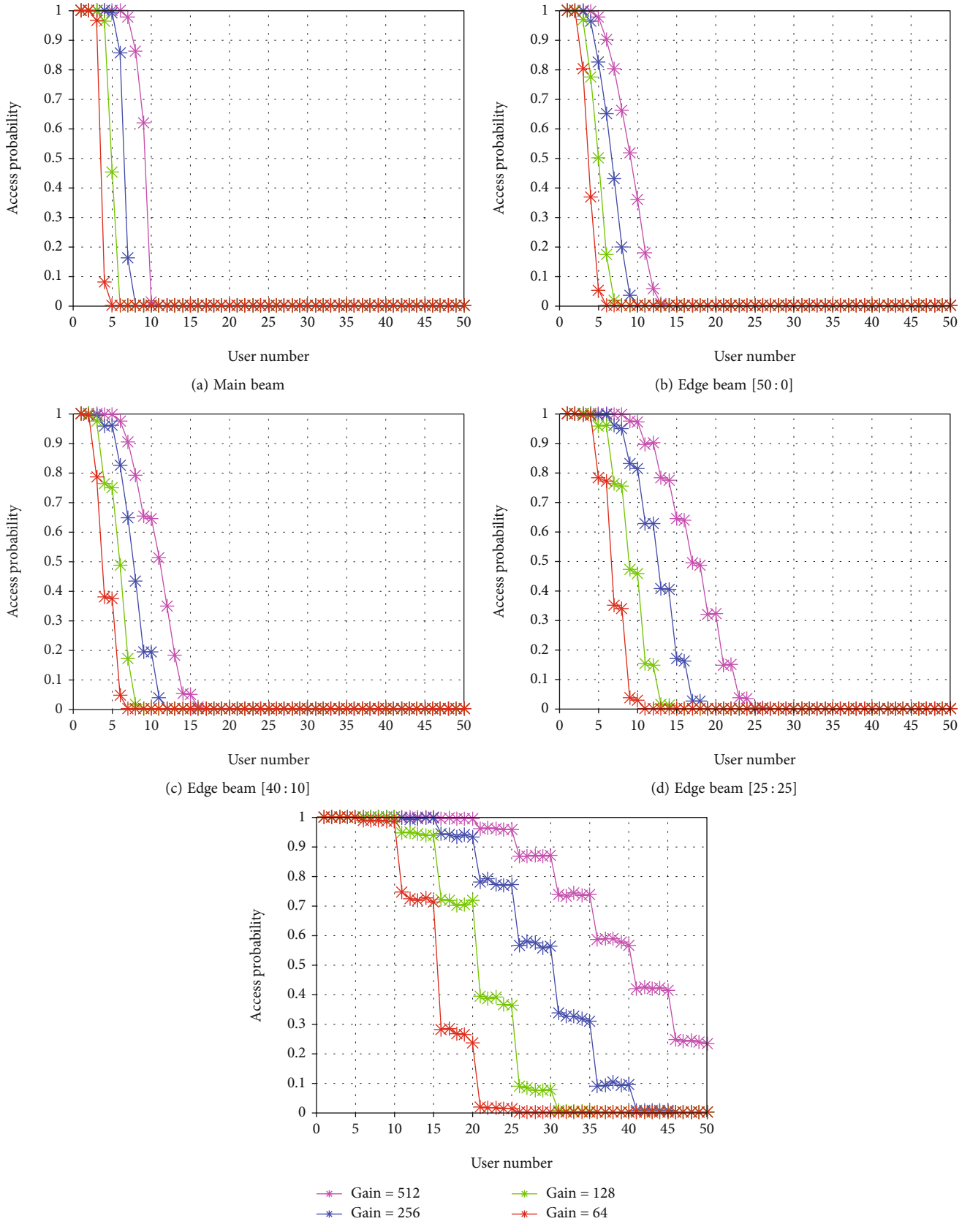

(a) Main beam

(b) Edge beam [50 : 0]

(c) Edge beam [40 : 10]

(d) Edge beam [25 : 25]

(e) Edge beam [10 : 40]

Figure 7: Terminal transmit power is $6 * P_0$.

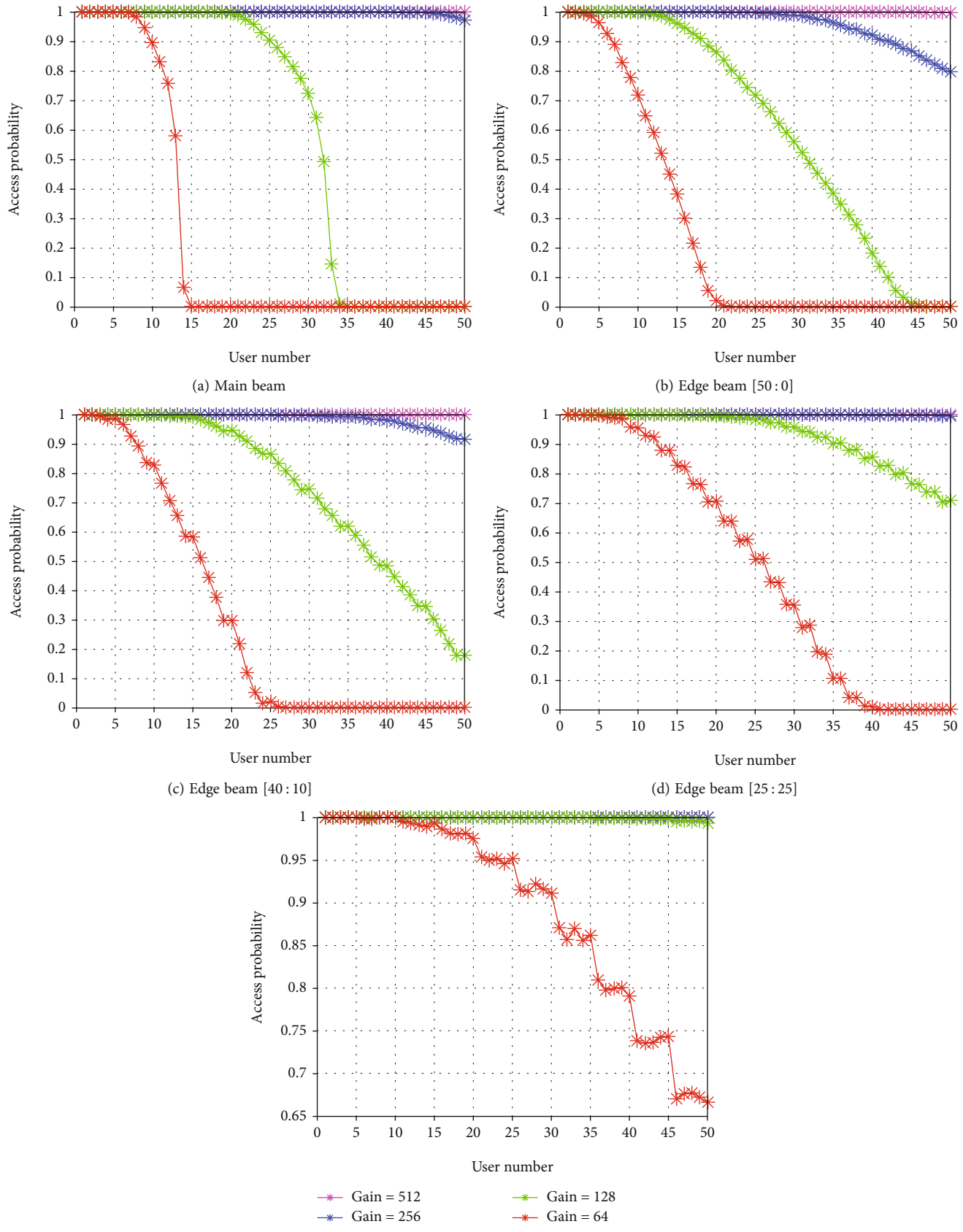

(a) Main beam

(b) Edge beam [50 : 0]

(c) Edge beam [40 : 10]

(d) Edge beam [25 : 25]

(e) Edge beam [10 : 40]

Figure 8: Terminal transmit power is P_0.

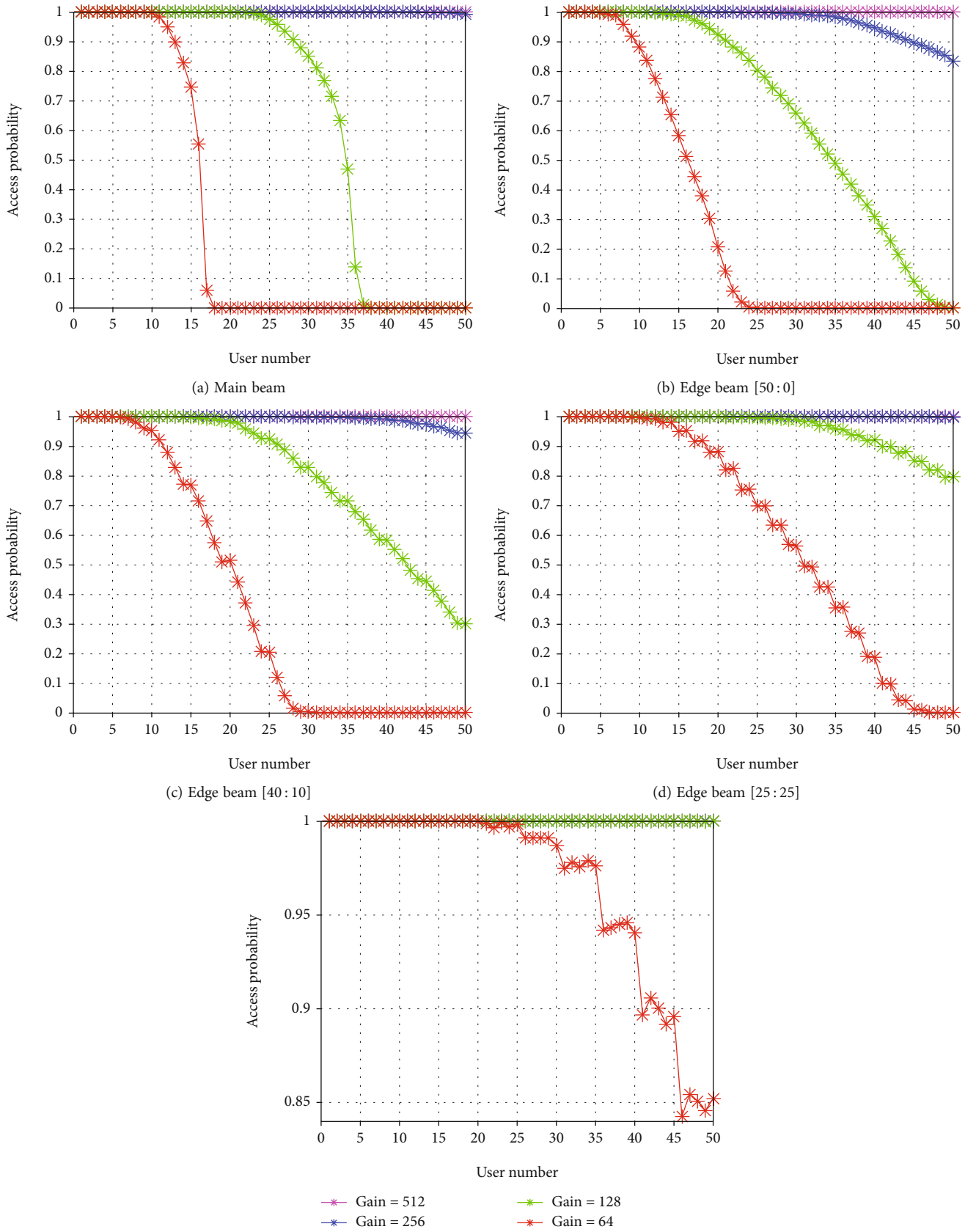

(a) Main beam

(b) Edge beam [50 : 0]

(c) Edge beam [40 : 10]

(d) Edge beam [25 : 25]

(e) Edge beam [10 : 40]

Figure 9: Terminal transmit power is $2 * P_0$.

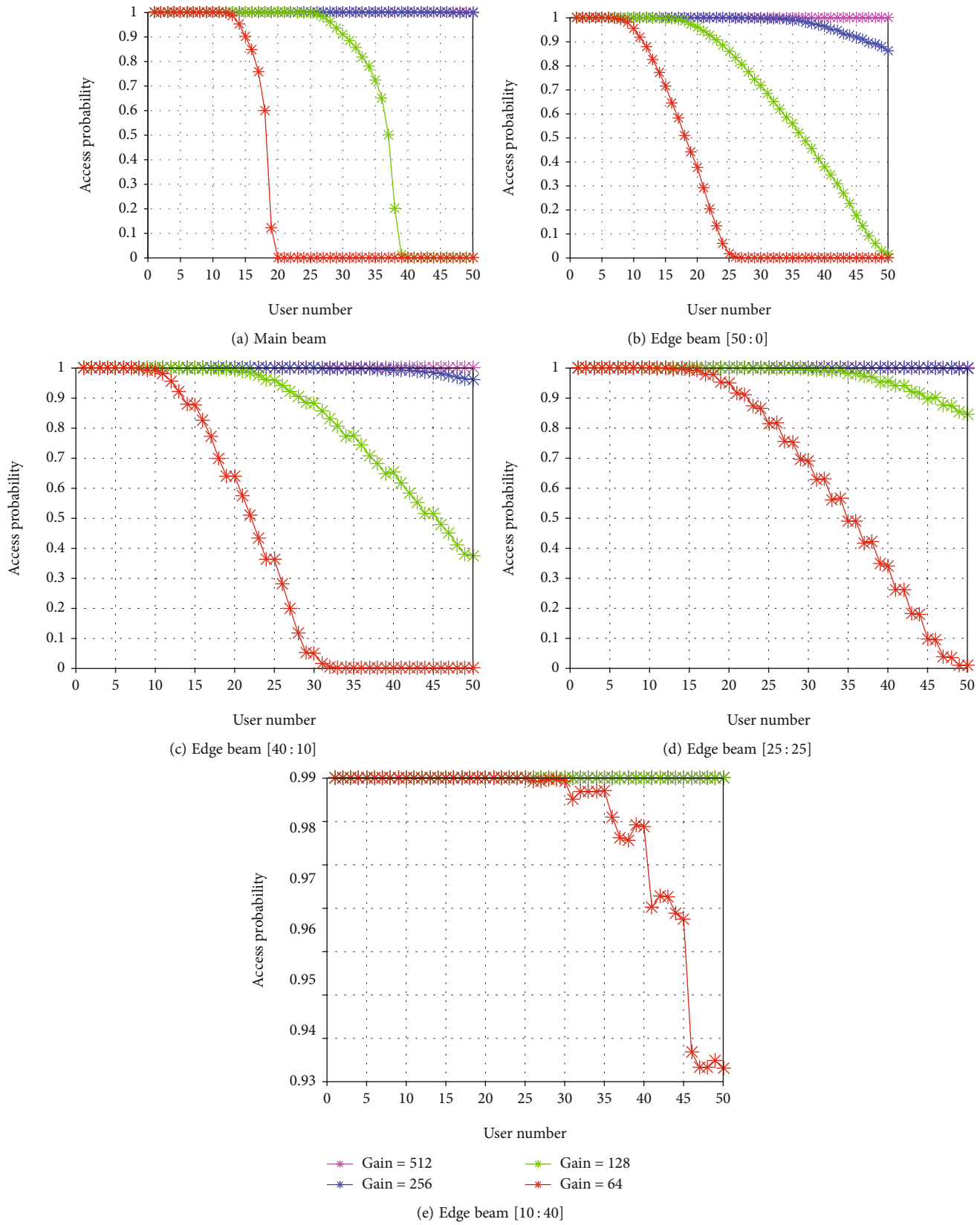

Figure 10: Terminal transmit power is $6 * P_0$.

beam with the same power, the user capacity increases as the gain increases. For example, under $6 * P_0$ power, the user capacity can be increased by about 20 under the same beam with different gains.

Finally, comparing the two sets of simulation results of the long spreading sequence and the short spreading sequence, it is not difficult to conclude that the use of the short spreading sequence can increase the user capacity. Taking P_0 power as an example, under the condition of maintaining a high access probability of 90%, the short code can access 7-8 more users than the long code. Although the short spreading sequence needs to consider the impact of collision on user access, the use of the short spreading sequence has better correlation characteristics than the long spreading sequence, which makes the user capacity of the short spreading sequence higher than that of the long spreading sequence.

5. Conclusion

This paper builds a multibeam satellite communication system model using CDMA. Since the user communication link of the multibeam satellite communication system is narrowband communication, the user capacity requirements are relatively high. In order to allocate user resources reasonably, the article simulates and analyzes capacity from collision probability and scene access probability. The results show that in the case of small spreading gain, the access probability of multiple users is generally low due to severe multiple access interference, while the probability of multiuser access is higher in the case of high gain. Due to the near-far effect, the user capacity of different beams is also different. The choice of long spreading sequence and short spreading sequence will also affect user capacity. The effect of sidelobe suppression and digital sampling on the MUI has not been considered in this paper, which will be discussed and studied as the follow-up work.

Data Availability

The data used to support the findings of this study are available from the corresponding author upon request.

Conflicts of Interest

The authors declare that they have no conflicts of interest.

Acknowledgments

This work is supported by the Youth Innovation Promotion Association CAS.

References

[1] C.-Q. Dai, M. Zhang, C. Li, J. Zhao, and Q. Chen, "QoE-aware intelligent satellite constellation design in satellite IoT," *IEEE Internet of Things Journal*, vol. 8, no. 3, pp. 4855–4867, 2020.

[2] Z. Shi, Z. Wu, Z. Kang, and X. Chen, "High and low orbit satellite mixed data transmission system application for power ubiquitous IoT," in *2019 IEEE 3rd Advanced Information Management, Communicates, Electronic and Automation Control Conference (IMCEC)*, pp. 1636–1642, Chongqing, China, 2019.

[3] X. Liu and X. Zhang, "NOMA-based resource allocation for cluster-based cognitive industrial internet of things," *IEEE Transactions on Industrial Informatics.*, vol. 16, no. 8, pp. 5379–5388, 2020.

[4] X. Liu, X. Zhai, W. Lu, and C. Wu, "QoS-guarantee resource allocation for multibeam satellite industrial internet of things with NOMA," *IEEE Transactions on Industrial Informatics.*, vol. 17, no. 3, pp. 2052–2061, 2021.

[5] X. Liu and X. Zhang, "Rate and energy efficiency improvements for 5G-based IoT with simultaneous transfer," *IEEE Internet of Things Journal*, vol. 6, no. 4, pp. 5971–5980, 2019.

[6] X. Liu, X. Zhang, M. Jia, L. Fan, W. Lu, and X. Zhai, "5G-based green broadband communication system design with simultaneous wireless information and power transfer," *Physical Communication*, vol. 28, pp. 130–137, 2018.

[7] H. Jiang, L. Li, H. Xian, Y. Hu, H. Huang, and J. Wang, "Crowd flow prediction for social internet-of-things systems based on the mobile network big data," *in IEEE Transactions on Computational Social Systems*, 2021.

[8] S. K. Routray, R. Tengshe, A. Javali, S. Sarkar, L. Sharma, and A. D. Ghosh, "Satellite based IoT for mission critical applications," in *2019 International Conference on Data Science and Communication (IconDSC)*, pp. 1–6, Bangalore, India, 2019.

[9] C. Fei, B. Zhao, W. Yu, and C. Wu, "Towards efficient data collection in space-based internet of things," *Sensors (Basel, Switzerland)*, vol. 19, no. 24, p. 5523, 2019.

[10] F. Li and K. Lam, "Resource optimization in satellite-based IoT," in *2020 International Conference on Artificial Intelligence in Information and Communication (ICAIIC)*, pp. 6–11, Fukuoka, Japan, 2020.

[11] M. J. M. Kiki, I. Iddi, and M. A. B. Olivero, "Analysis of multiple access approaches on IoT via LEO satellite," in *2020 IEEE 11th International Conference on Software Engineering and Service Science (ICSESS)*, pp. 175–179, Beijing, China, 2020.

[12] Y. He, Y. Jia, and X. Zhong, "A traffic-awareness dynamic resource allocation scheme based on multi-objective optimization in multi-beam mobile satellite communication systems," *International Journal of Distributed Sensor Networks*, vol. 13, no. 8, 2017.

[13] X. Lin, Y. Mao, B. Zhao, and M. Xu, "Design of satellite borne DBF multi-beam receiving system," in *2018 Eighth International Conference on Instrumentation & Measurement, Computer, Communication and Control (IMCCC)*, pp. 30–33, Harbin, China, 2018.

[14] X. Hu, X. Luan, S. Ren, and J. Wu, "Propagation delays computation in GEO multi-beam satellite communications system," in *2012 International Conference on Systems and Informatics (ICSAI2012)*pp. 1631–1634, Yantai, China, 2012.

[15] S. Ren, X. Luan, R. Zhu, and J. Wu, "Multi-beam joint detection combination for TD-SCDMA compatible mobile satellite communication system," in *2012 International Conference on Control Engineering and Communication Technology*pp. 944–947, Shenyang, China, 2012.

[16] L. You, A. Liu, W. Wang, and X. Gao, "Outage constrained robust multigroup multicast beamforming for multi-beam satellite communication systems," *in IEEE Wireless Communications Letters*, vol. 8, no. 2, pp. 352–355, 2019.

[17] P. Viswanath and V. Anantharam, "User capacity of a power controlled CDMA system with multiple base stations," in *Proceedings of the 1999 IEEE Information Theory and Communications Workshop (Cat. No. 99EX253)*, pp. 21–23, Kruger National Park, South Africa, 1999.

[18] P. Kabir, M. H. Shafinia, and F. Marvasti, "Capacity bounds of finite dimensional CDMA systems with power allocation, fading, and near-far effects," *in IEEE Communications Letters*, vol. 17, no. 1, pp. 15–18, 2013.

[19] J. O. Mark, M. N. M. Saad, and B. B. Samir, "Average BER perfomance and spectral efficiency for MIMO orthogonal MC DS-CDMA system over Nakagami-m fading channels," in *2011 National Postgraduate Conference*, pp. 1–6, Perak, Malaysia, 2011.

[20] Z. Qi, X. Jing, and S. You, "The capacity analysis on a HAPS-CDMA system based on the platform displacement model," in *2010 2nd IEEE InternationalConference on Network Infrastructure and Digital Content*, pp. 870–874, Beijing, China, 2010.

[21] J. Dai, Y. Sun, and Y. Qin, "Power control with QoS-constraints for maximizing the sum capacity of reverse-link CDMA system," in *Proceedings of the 30th Chinese Control Conference*, pp. 4402–4405, Yantai, China, 2011.

[22] R. Kabir, M. M. Haque, and M. Rahaman, "Channel capacity and bit error rate analysis of non-uniform type M-ary optical CDMA in presence of self phase modulation and dispersion," in *8th International Conference on Electrical and Computer Engineering*, pp. 421–424, Dhaka, Bangladesh, 2014.

[23] M. J. Arsehdogad and M. Ghorbani, "A new survey for capacity of CDMA systems," in *2012 IEEE International Conference on Information Science and Technology*, pp. 889–892, Wuhan, China, 2012.

[24] O. Soykalan, A. Rizaner, and A. H. Ulusoy, "Capacity and performance comparison of IDMA and CDMA systems," in *2013 21st Signal Processing and Communications Applications Conference (SIU)*, pp. 1–4, Haspolat, Turkey, 2013.

[25] T. Song, K. Zhou, and T. Li, "CDMA system design and capacity analysis under disguised jamming," *in IEEE Transactions on Information Forensics and Security*, vol. 11, no. 11, pp. 2487–2498, 2016.